

Engineering Iridium-Containing Metal-organic Molecular Capsule for Induced-Fit Geometrical Conversion and Dual Catalysis

Xuezha Li, Jinguo Wu, Liyong Chen, Xiaoming Zhong, Cheng He,* Rong Zhang and Chunying Duan

E-mail: hecheng@dlut.edu.cn.

1. General Information

2. Syntheses and Characterizations

2.1 Synthesis of *fac*-Ir-NH₂

2.2 Synthesis of Ir-Co1

2.3 Synthesis of Ir-Co2

2.4 Synthesis of 2-Acyl Pyridines

3. Photoredox Reactions

4. Mechanistic Experiments

4.1 Control experiments

4.2 ESI-MS tracking experiment based on the coordination of Ir-Co1 with CO₃²⁻

4.3 ESI-MS tracking experiment based on the coordination of Ir-Co1 with 1a

4.4 UV-vis spectra of 1a, Ir-Co1, Ir-Co2 and the related titration experiments

4.5 Possible catalytic mechanism

5. Single-Crystal X-Ray Diffraction Studies

6. NMR Spectra

7. References

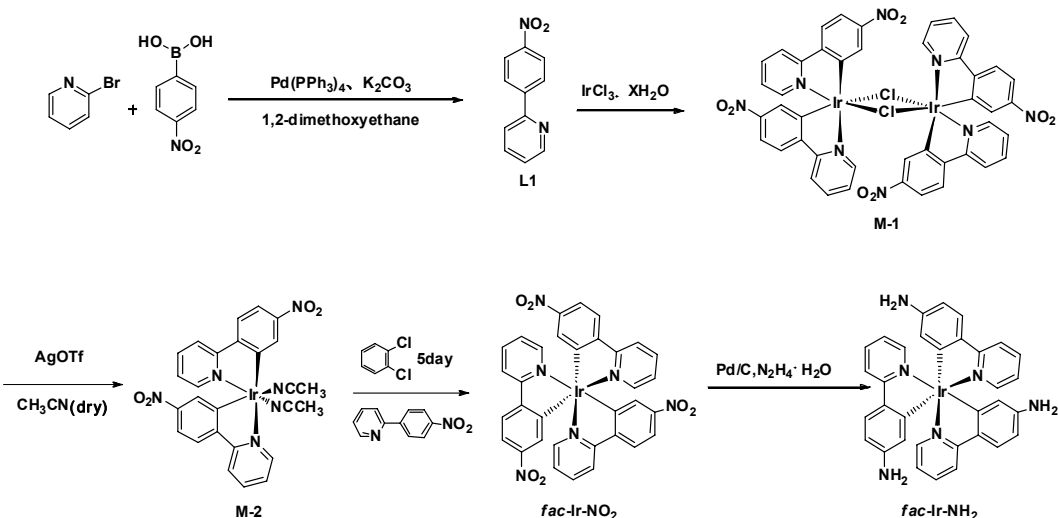
1. General Information

All reactions were carried out under an atmosphere of argon or nitrogen with magnetic stirring. Catalysis reactions were performed in a Schlenk tube (10 mL). As light sources served a 26 W compact fluorescence lamp. Solvents were distilled under nitrogen from calcium hydride (CH_3CN) or magnesium turnings/iodine (MeOH). Reagents that were purchased from commercial suppliers were used without further purification. ^1H NMR and ^{13}C NMR spectra were recorded on Bruker Avance 400 III (400 MHz) spectrometers at ambient temperature. NMR standards were used as follows: ^1H NMR spectroscopy: $\delta = 7.26$ ppm (CDCl_3), $\delta = 5.32$ ppm (CD_2Cl_2). ESI mass spectra were carried out on ESI-MS spectrometer using methanol as mobile phase. UV-vis spectra were measured on a HP 8453 spectrometer. Abbreviations: ppy = 2-(4-Nitrophenyl)-pyridine; nm = nanometres; min = minute(s); h = hour(s); rt = room temperature (20 °C).

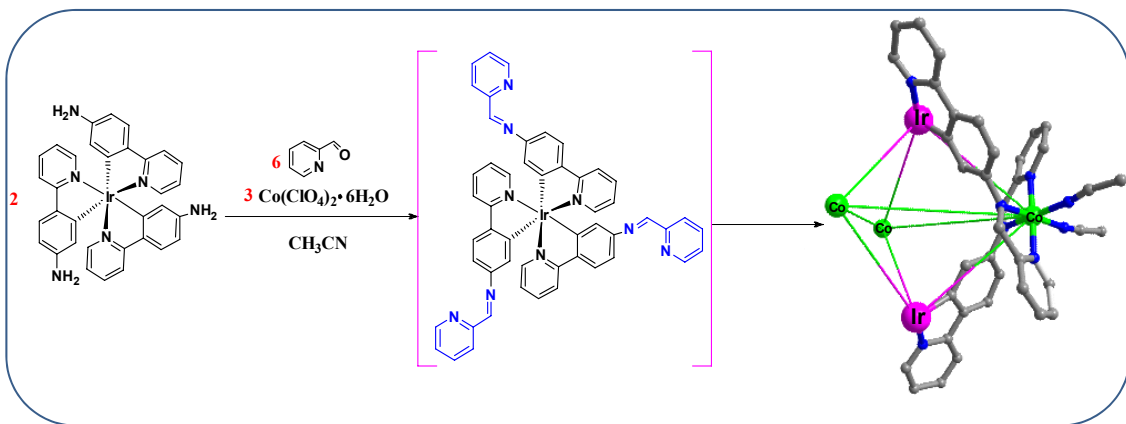
2. Syntheses and Characterizations

2.1 Synthesis of *fac*-Ir-NH₂

Ligand *fac*-Ir-NH₂ was synthesized according to our reported procedure. [S1]



Scheme S1 Synthesis of *fac*-Ir-NH₂



2.2. Synthesis of compound Ir-Co1

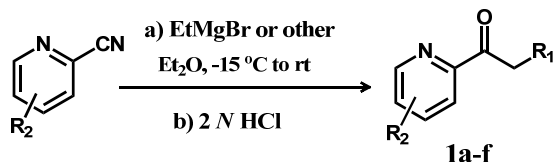
To a Schlenk tube was added *fac*-Ir-NH₂ (35 mg, 0.05 mmol, 2 equiv.), 2-formylpyridine (15 μ L, 0.15 mmol, 6 equiv.), Co(ClO₄)₂·6H₂O (28 mg, 0.075 mmol, 3 equiv.) in acetonitrile (40 mL). The solution was refluxed for 24 h, diethyl ether was slowly diffused into the aforementioned solution and formed the dark wine crystals (yield 80%, based on the crystal dried vacuum). ESI-MS m/z = 577.4005 [Co₃(Ir-PY)₂·2ClO₄⁻]⁴⁺, 802.8463 [Co₃(Ir-PY)₂·3ClO₄⁻]³⁺ and 1254.7279 [Co₃(Ir-PY)₂·4ClO₄⁻]²⁺. Anal. Calc. for [Co₃(C₅₁H₃₆N₉Ir)₂(ClO₄)₆(CH₃CN)₆(H₂O)₂]: H, 3.17; C, 45.79; N, 11.24. Found: H, 3.11; C, 46.08; N, 11.86.

2.3. Synthesis of compound Ir-Co2

An aqueous solution of $(\text{NH}_4)_2\text{CO}_3$ (200 μL , 1×10^{-2} M, 2.0 equiv.) was added dropwise to acetonitrile solution of **Ir-Co1** (10 mL, 1×10^{-4} M). The mixture was stirred at room temperature overnight. Then the solution was diffused with diethyl ether, the wine red crystals was obtained (yield 91%, based on the crystal dried vacuum). ESI-MS: $[\text{Co}_3(\text{Ir-PY})_2\cdot\text{CO}_3^{2-}]^{4+}$ 542.8960, $[\text{Co}_3(\text{Ir-PY})_2\cdot\text{CO}_3^{2-}\cdot\text{ClO}_4^-]^{3+}$ 756.8491, $[\text{Co}_3(\text{Ir-PY})_2\cdot\text{CO}_3^{2-}\cdot 2\text{ClO}_4^-]^{2+}$ 1184.7421. Anal. Calc. for $[\text{Co}_3(\text{C}_{51}\text{H}_{36}\text{N}_9\text{Ir})_2(\text{CO}_3)(\text{ClO}_4)_4(\text{CH}_3\text{CN})_2(\text{H}_2\text{O})]$: H, 3.02; C, 48.15; N, 10.50. Found: H, 2.97; C, 48.38; N, 10.29.

2.4 Synthesis of 2-Acyl Pyridines

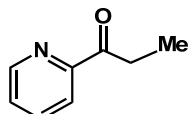
All 2-acyl pyridines (**1a-f**) were synthesized according to reported procedures with some modifications.^{[S2][S3]}



General procedure for the synthesis of 2-acyl pyridines.

To a solution of the corresponding 2-pyridinecarbonitrile (1.0 eq) in Et₂O (0.5 M) at -15 °C were added ethylmagnesium bromide or propylmagnesium bromide, isopropylmagnesium bromide, pentylmagnesium bromide, (1.2 eq, 1.0 M in THF). The reaction mixture was stirred at -15 °C for 1 h, then allowed to warm to room temperature and stirred for a further 4.0 h. The mixture was added 2 N HCl (2.4 eq) and stirred at room temperature for 30 min. The reaction was neutralized with 2 N NaOH to pH 8 and diluted with EtOAc. The organic layer was washed with aqueous saturated NaHCO₃ and brine (60 mL). The combined organic layers were dried over anhydrous Na₂SO₄, filtered, and concentrated under reduced pressure. The residue was purified by flash chromatography on silica gel (EtOAc/hexane = 1:10) to obtain the pure compounds **1a-f**.

1-(Pyridin-2-yl)propan-1-one (**1a**)

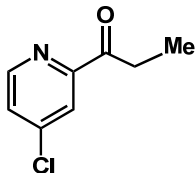


Following the general procedure, 2-pyridinecarbonitrile (1.5 mL, 16.0 mmol) with ethylmagnesium bromide (19.2 mL, 19.2 mmol) was converted to 2-acyl pyridine **1a** (1.77 g,

13.1 mmol, yield: 82%) as a colorless oil.

¹H NMR (400 MHz, CDCl₃) δ 8.61 (m, 1H), 7.98-7.96 (m, 1H), 7.76 (td, *J* = 6.0, 1.2 Hz, 1H), 7.39 (m, 1H), 3.17 (q, *J* = 5.6 Hz, 2H), 1.14 (t, *J* = 5.6 Hz, 3H).

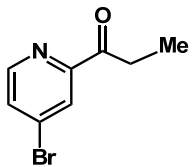
1-(4-Chloropyridin-2-yl)propan-1-one (1b)



Following the general procedure, 4-chloro-2-pyridinecarbonitrile (1.39 g, 10 mmol) with ethylmagnesium bromide (12 mL, 12 mmol) was converted to 2-acyl pyridine **1b** (1.454 g, 8.6 mmol, yield: 86%) as a pale yellow oil.

¹H NMR (400 MHz, CDCl₃) δ 8.52 (d, *J* = 4.0 Hz, 1H), 7.95 (dd, *J* = 1.6, 0.4 Hz, 1H), 7.42 (dd, *J* = 4.4, 1.6 Hz, 1H), 3.14 (q, *J* = 5.6 Hz, 2H), 1.14 (t, *J* = 5.6 Hz, 3H).

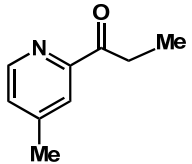
1-(4-Bromopyridin-2-yl)propan-1-one (1c)



Following the general procedure, 4-bromo-2-pyridinecarbonitrile (1.83 g, 10 mmol) with ethylmagnesium bromide (12 mL, 12 mmol) was converted to 2-acyl pyridine **1c** (1.725 g, 8.1 mmol, yield: 81%) as a white solid.

¹H NMR (400 MHz, CDCl₃) δ 8.44 (d, *J* = 4.4 Hz, 1H), 8.14 (d, *J* = 1.6 Hz, 1H), 7.59 (dd, *J* = 4.0, 1.6 Hz, 1H), 3.17 (q, *J* = 5.6 Hz, 2H), 1.38-1.11 (t, *J* = 6.0 Hz, 3H).

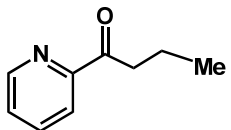
1-(4-Methylpyridin-2-yl)propan-1-one (1d)



Following the general procedure, 4-methyl-2-pyridinecarbonitrile (1.18g, 10 mmol) with ethylmagnesium bromide (12 mL, 12 mmol) was converted to 2-acyl pyridine **1d** (1.297g, 8.7 mmol, yield: 87%) as a colorless oil.

¹H NMR (400 MHz, CDCl₃) δ 8.48 (d, *J* = 4.0 Hz, 1H), 7.82 (s, 1H), 7.23 (d, *J* = 3.2 Hz, 1H), 3.19 (q, *J* = 5.6 Hz, 2H), 2.38 (s, 3H), 1.70 (t, *J* = 5.6 Hz, 3H).

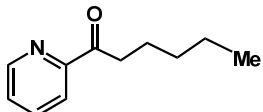
1-(pyridin-2-yl)butan-1-one(1e)



Following the general procedure, 2-pyridinecarbonitrile (0.94 mL, 10 mmol) with propylmagnesium bromide (12 mL, 12 mmol) was converted to 2-acyl pyridine **1e** (1.342 g, 9.0 mmol, yield: 90%) as a colorless oil.

¹H NMR (400 MHz, CDCl₃) δ 8.62 (d, *J* = 3.6 Hz, 1H), 7.97 (d, *J* = 6.4, 1H), 7.76 (td, *J* = 6.0, 1.2 Hz, 1H), 7.41-7.38(m, 1H), 3.13(t, *J* = 5.6 Hz, 2H), 1.73-1.68 (m, 2H), 0.95 (t, *J* = 6.0 Hz, 3H).

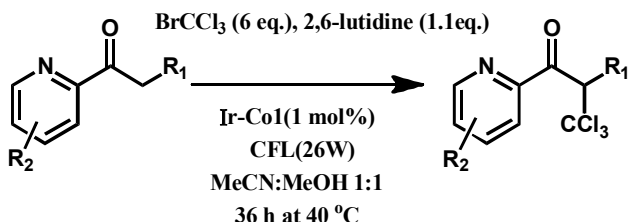
1-(pyridin-2-yl)hexan-1-one(1f)



Following the general procedure, 2-pyridinecarbonitrile (0.94 mL, 10 mmol) with pentylmagnesium bromide (12 mL, 12 mmol) was converted to 2-acyl pyridine **1f** (1.541g, 8.7 mmol, yield: 87%) as a colorless oil.

¹H NMR (400 MHz, CDCl₃) δ 8.56-8.54 (m, 1H), 7.92-7.89 (m, 1H), 7.70 (td, *J* = 8.0, 2.0 Hz, 1H), 7.35-7.31(m, 1H), 3.08(t, *J* = 6.8 Hz, 2H), 1.64-1.60 (m, 2H), 1.28-1.22(m, 4H), 0.80-0.76 (m, 3H).

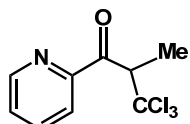
3. Photoredox Reactions



General procedure: α -trichloromethylation of 2-acyl pyridines.

A dried 10 mL Schlenk tube was charged with the catalyst **Ir-Co1** (1 mol%) and the corresponding 2-acyl pyridine **1a-f** (0.1 mmol, 1.0 eq). The tube was purged with nitrogen and MeOH/MeCN (1:1, 0.5 mL) was added *via* syringe, followed by 2,6-lutidine (13.0 μ L, 0.11 mmol, 1.1 eq) and bromotrichloromethane (60.0 μ L, 0.6 mmol, 6.0 eq). The reaction mixture was degassed *via* freeze-pump-thaw for three cycles. After the mixture was thoroughly degassed, the vial was sealed and positioned approximately 5 cm from a 26 W compact fluorescence lamp. The reaction was stirred at 40 °C (silicone oil bath) for the indicated time (monitored by TLC) under nitrogen atmosphere. Afterwards, the mixture was concentrated under reduced pressure. The residue was purified by flash chromatography on silica gel to afford the products **2a-f**.

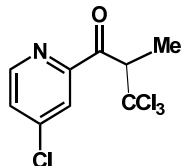
3,3,3-Trichloro-2-methyl-1-(pyridin-2-yl)propan-1-one (2a)



Starting from 2-acyl pyridine **1a** (14.0 mg, 0.10 mmol) according to the general procedure to give **2a** as a colorless oil (22.8 mg, 0.091 mmol, yield: 91%).

¹H NMR (400 MHz, CDCl₃) δ 8.71 (d, *J* = 3.6 Hz, 1H), 8.11 (d, *J* = 6.4, 1H), 7.90-7.87 (m, 1H), 7.54-7.51 (m, 1H), 5.66 (q, *J* = 5.6 Hz, 1H), 1.62 (d, *J* = 5.2 Hz, 3H).

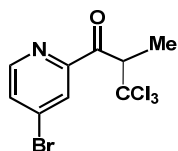
3,3,3-Trichloro-1-(4-chloropyridin-2-yl)-2-methylpropan-1-one (2b)



Starting from 2-acyl pyridine **1b** (17 mg, 0.10 mmol) according to the general procedure to give **2b** as a colorless oil (26.2 mg, 0.092 mmol, yield: 92%).

¹H NMR (400 MHz, CDCl₃) δ 8.61 (d, *J* = 4.4 Hz, 1H), 8.08 (d, *J* = 1.6 Hz, 1H), 7.53 (dd, *J* = 4.4, 1.6 Hz, 1H), 5.59 (q, *J* = 5.6 Hz, 1H), 1.61 (d, *J* = 5.6 Hz, 3H).

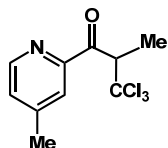
1-(4-Bromopyridin-2-yl)-3,3,3-trichloro-2-methylpropan-1-one(2c)



Starting from 2-acyl pyridine **1c** (21.3 mg, 0.10 mmol) according to the general procedure to give **2c** as a colorless oil (31.6 mg, 0.096 mmol, yield: 96%).

¹H NMR (400 MHz, CDCl₃) δ 8.53 (d, *J* = 5.2 Hz, 1H), 8.25 (d, *J* = 1.6 Hz, 1H), 7.69 (dd, *J* = 5.2, 2.0 Hz, 1H), 5.59 (q, *J* = 7.2 Hz, 1H), 1.61 (d, *J* = 7.2 Hz, 3H).

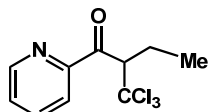
3,3,3-Trichloro-2-methyl-1-(4-methylpyridin-2-yl)propan-1-one (2d)



Starting from 2-acyl pyridine **1d** (14.9 mg, 0.10 mmol) according to the general procedure to give **2d** as a colorless oil (24.5 mg, 0.093 mmol, yield: 93%).

¹H NMR (400 MHz, CDCl₃) δ 8.56 (d, *J* = 5.2 Hz, 1H), 7.93 (s, 1H), 7.34 (d, *J* = 4.8 Hz, 1H), 5.56 (q, *J* = 6.8 Hz, 1H), 2.45 (s, 3H), 1.61 (d, *J* = 6.8 Hz, 3H).

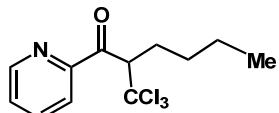
3,3,3-Trichloro-2-ethyl-1-(pyridin-2-yl)propan-1-one (2e)



Starting from 2-acyl pyridine **1e** (14.9 mg, 0.10 mmol) according to the general procedure to give **2e** as a colorless oil (22.8 mg, 0.086 mmol, yield: 86%).

¹H NMR (400 MHz, CDCl₃) δ 8.75-8.74 (m, 1H), 8.13 (d, *J* = 8.0 Hz, 1H), 7.88 (td, *J* = 7.6, 1.6 Hz, 1H), 7.54-7.50 (m, 1H), 5.71 (dd, *J* = 10.0, 3.6 Hz, 1H), 2.30-2.18 (m, 1H), 0.91(t, *J* = 7.6 Hz, 3H).

3,3,3-Trichloro-2-n-butyl-1-(pyridin-2-yl)propan-1-one (2f)



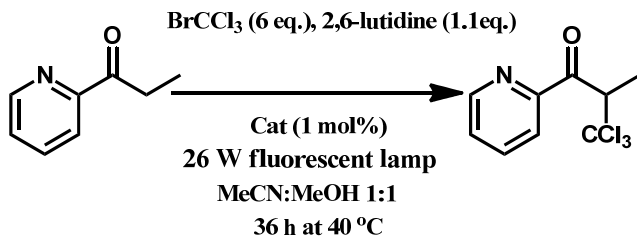
Starting from 2-acyl pyridine **1f** (21.3 mg, 0.10 mmol) according to the general procedure to give **2f** as a colorless oil (26.4 mg, 0.09 mmol, yield: 90%).

¹H NMR (400 MHz, CDCl₃) δ 8.75-8.73 (m, 1H), 8.12 (dt, *J* = 8.0, 1.2 Hz, 1H), 7.87 (td, *J* = 7.6, 0.8 Hz, 1H), 7.53-7.50 (m, 1H), 5.75 (dd, *J* = 10.8, 3.2 Hz, 1H), 2.29-2.07 (m, 2H), 1.42-1.10 (m, 4H), 0.83 (t, *J* = 6.8 Hz, 3H).

4. Mechanistic Experiments

4.1 Control Experiments

Table S1 Control experiments for the visible light activated trichloromethylation of **1a**^a

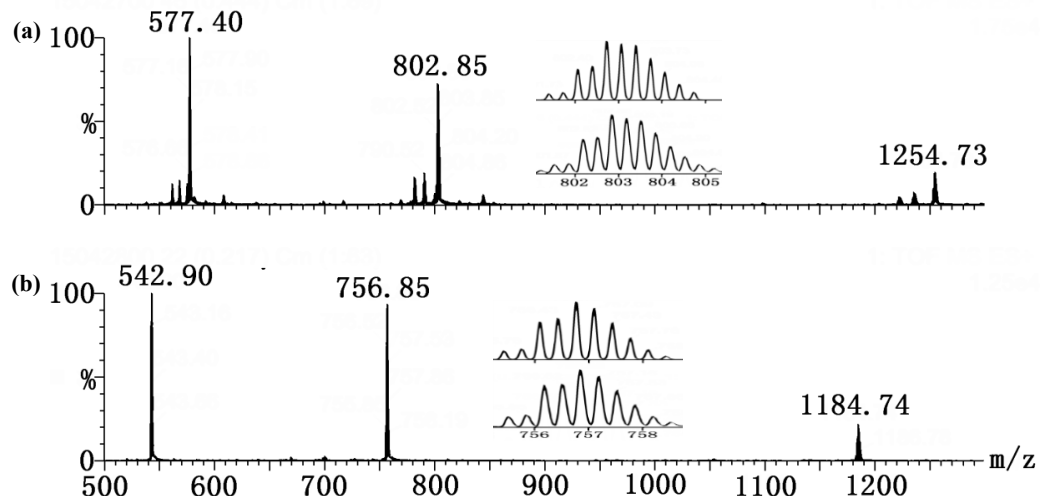


Entry	Catalyst	Addition	yield
1	NO	In dark	0
2	NO		0
3	Ir-Co1	In dark	<5%
4	<i>fac</i> -NH ₂ + Co(ClO ₄) ₂ ·6H ₂ O		<10%
5	<i>fac</i> -NH ₂		trace
6	Co(ClO ₄) ₂ ·6H ₂ O		trace
7	Ir-Co2		6%

^a Reaction conditions: 2-acylpyridine **1a** and BrCCl₃ (6 equiv.), 2,6-lutidine (1.1 equiv.) with catalyst (1 mol%) in MeCN/MeOH 1:1 at 40 °C for 36 h under argon. Light source: 26 W compact fluorescence lamp.

4.2 ESI-MS tracking experiment based on the coordination of Ir-Co1 with CO_3^{2-}

The ESI-MS of **Ir-Co1** in acetonitrile solution was obtained (Fig. S1a). To this Host solution **Ir-Co1**(1×10^{-4} M, 1 mL) was added 20 μL $(\text{NH}_4)_2\text{CO}_3$ (1×10^{-2} M, H_2O , 2.0 equiv.). The mixture was stirred at room temperature overnight. The species of **Ir-Co1** coordinated with CO_3^{2-} was found in the ESI-MS spectra (Fig. S1b).

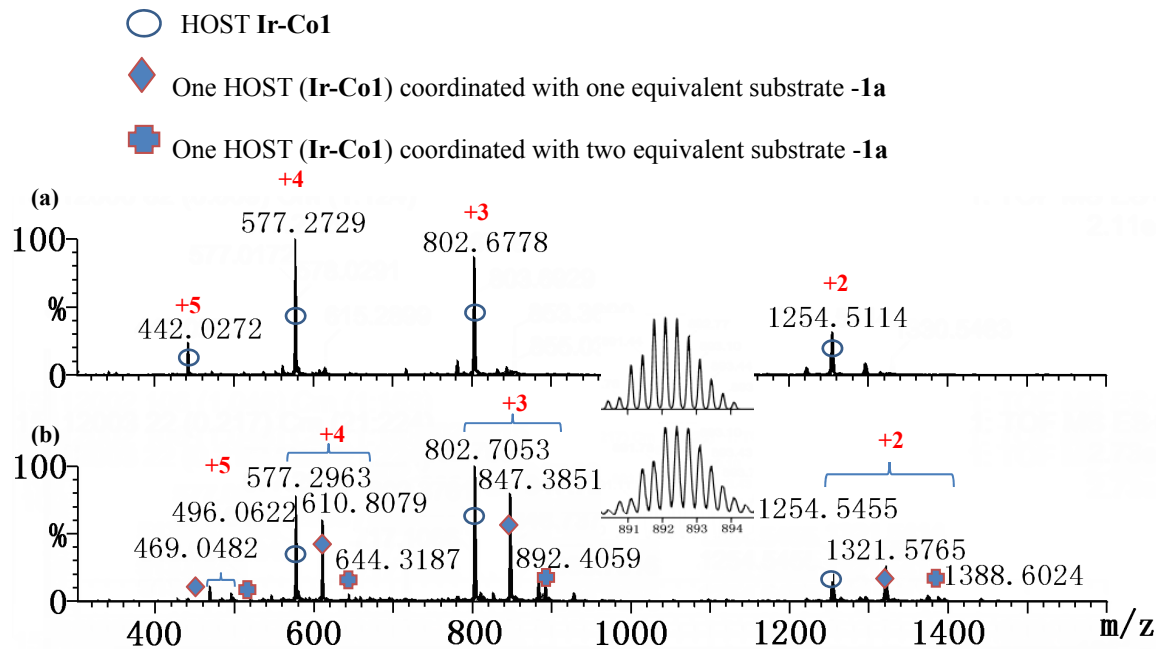


Peak number	Ex-Value	Th-Value	Specie Assigned
1	542.8961	542.8427	$[\text{Co}_3(\text{Ir-PY})_2 \supset \text{CO}_3^{2-}]^{4+}$
2	765.8491	756.7615	$[\text{Co}_3(\text{Ir-PY})_2 \supset \text{CO}_3^{2-} \cdot \text{ClO}_4]^{3+}$
3	1184.7421	1184.6286	$[\text{Co}_3(\text{Ir-PY})_2 \supset \text{CO}_3^{2-} \cdot (\text{ClO}_4^-)_2]^{2+}$

Figure S1 ESI-MS spectra of the tracking experiment based on the coordination of **Ir-Co1** with CO_3^{2-}

4.3 ESI-MS tracking experiment based on the coordination of Ir-Co1 with 1a

The ESI-MS of **Ir-Co1** in acetonitrile solution was obtained (Fig. S2a). To this Host solution **Ir-Co1**(1×10^{-4} M, 1 mL) was added 60 μ L **1a** (1×10^{-2} M, 2.0 equiv. for each Co^{II} center). The mixture was stirred at room temperature overnight. The species of **Ir-Co1** coordinated with **1a** was found in the ESI-MS spectra (Fig. S2b).



Peak number	Ex-Value	Th-Value	Specie Assigned
1	610.8079	611.0801	$[\text{Co}_3(\text{Ir-PY})_2(\text{ClO}_4^-)_2(\mathbf{1a})]^{4+}$
2	644.3187	644.8472	$[\text{Co}_3(\text{Ir-PY})_2(\text{ClO}_4^-)_2(\mathbf{1a})_2]^{4+}$
3	847.3851	847.7575	$[\text{Co}_3(\text{Ir-PY})_2(\text{ClO}_4^-)_3(\mathbf{1a})]^{3+}$
4	892.7529	893.1151	$[\text{Co}_3(\text{Ir-PY})_2(\text{ClO}_4^-)_3(\mathbf{1a})_2]^{3+}$
5	1321.5765	1322.1198	$[\text{Co}_3(\text{Ir-PY})_2(\text{ClO}_4^-)_4(\mathbf{1a})]^{2+}$
6	1388.6024	1389.6536	$[\text{Co}_3(\text{Ir-PY})_2(\text{ClO}_4^-)_4(\mathbf{1a})_2]^{2+}$

Figure S2 ESI-MS spectra of the tracking experiment based on the coordination of **Ir-Co1** with **1a**

4.4 UV-vis spectra of **1a**, **Ir-Co1** and **Ir-Co2** the related titration experiments

4.4.1 UV-vis spectra of **1a** (1×10^{-5} - 1×10^{-4} M, CH₃CN), **Ir-Co1** (1×10^{-5} M, CH₃CN) and **Ir-Co2** (1×10^{-5} M, CH₃CN).

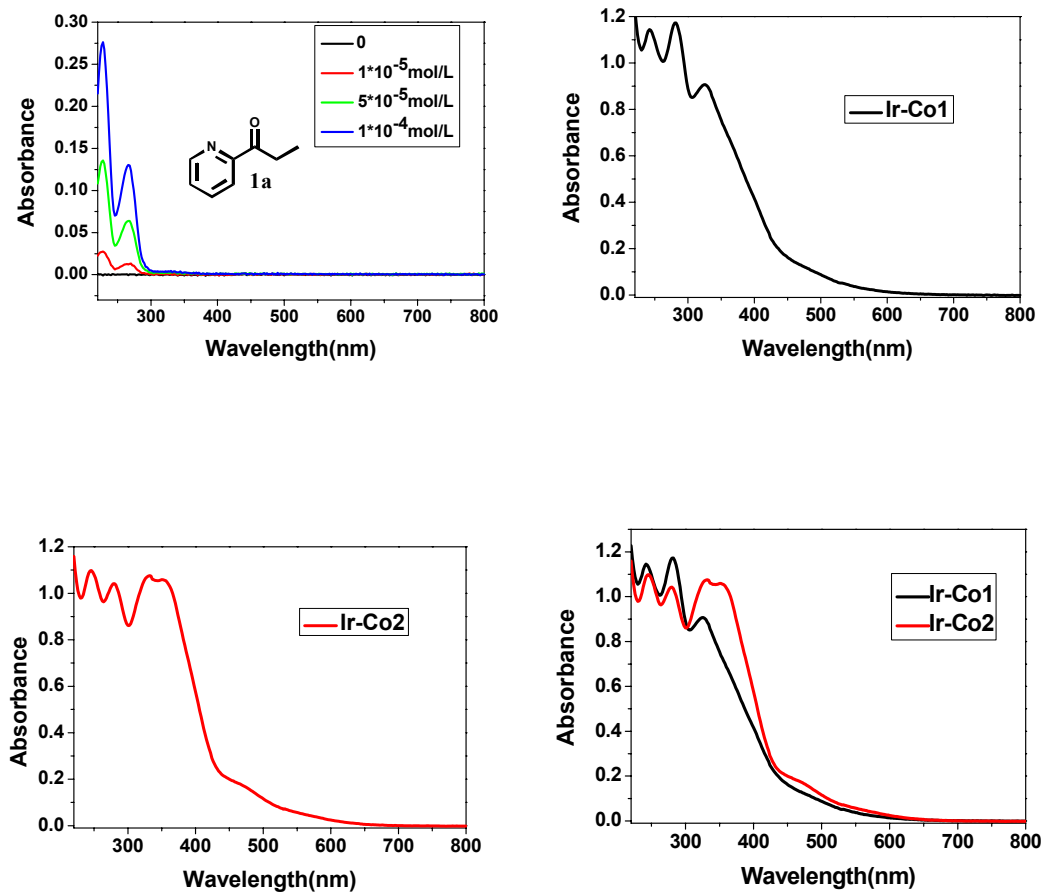


Figure S3 UV-vis spectra of **1a**, **Ir-Co1** and **Ir-Co2**

4.4.2 UV-vis titration experiment of Ir-Co1 upon addition of 1.0 to 4.0 equiv. of CO_3^{2-} (Induced-Fit Recognition Behavior).

Added only 1.0 equiv. carbonate anions to the solution of capsule **Ir-Co1** (1×10^{-5} M, CH_3CN), the absorbance spectra dramatically changed to a balance state in a very short time. The 243 nm, 281 nm absorbance intensity decreased and the 300-430 nm range absorbance intensity increased gradually (red line). Especially, 430-650 nm region associated with MLCT transition for the low energy band absorbance intensity also increased gradually to a balance. Added another portion of carbonate anions did not affect the absorbance of the solution.

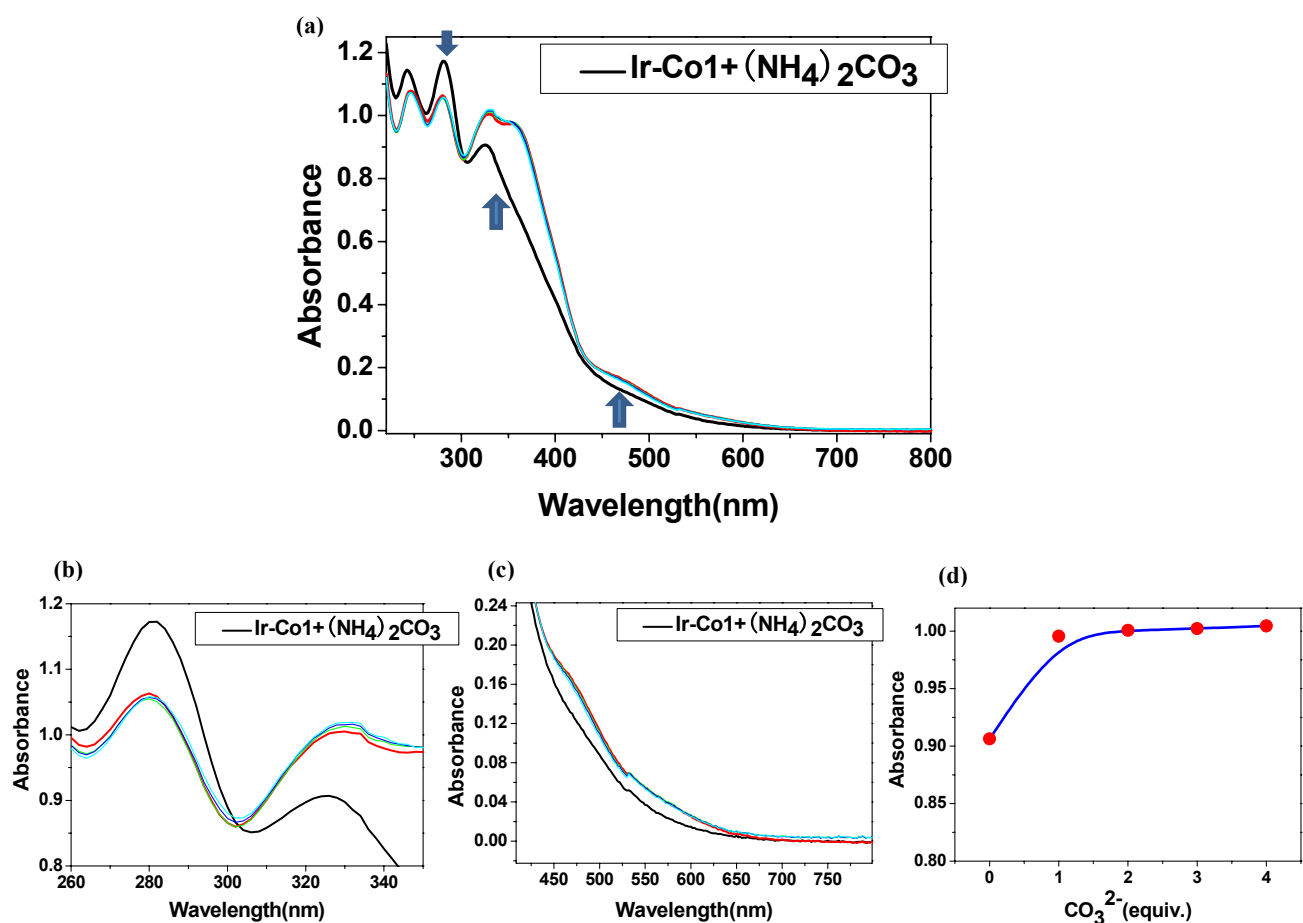


Figure S4 (a) Family of the differentiate UV-vis absorption spectra of **Ir-Co1**(10 μM , black line) in CH_3CN upon addition of 1.0 equiv. of $(\text{NH}_4)_2\text{CO}_3$ (red line) and excess $(\text{NH}_4)_2\text{CO}_3$ (2.0 to 4.0 equiv.), respectively; (b) The range of 260-350 nm; (c) The range of 408-798 nm; (d) The UV-vis absorption intensity tracing at 324 nm.

4.4.3 UV-vis titration experiment of Ir-Co1 upon addition of 1.2 to 12.0 equiv. of 1a

When 3.0 equiv. 2-acylpyridine (**1a**) was added to the solution of capsule **Ir-Co1** (1×10^{-5} M, CH₃CN), the 275 nm absorbance intensity decreased and the 300-400 nm, 420-500 nm range absorbance intensity increased gradually. Continues adding the **1a** (6.0-12.0 equiv.) only caused the absorbance intensity increase of itself, which indicated the bounding process was truly happened.

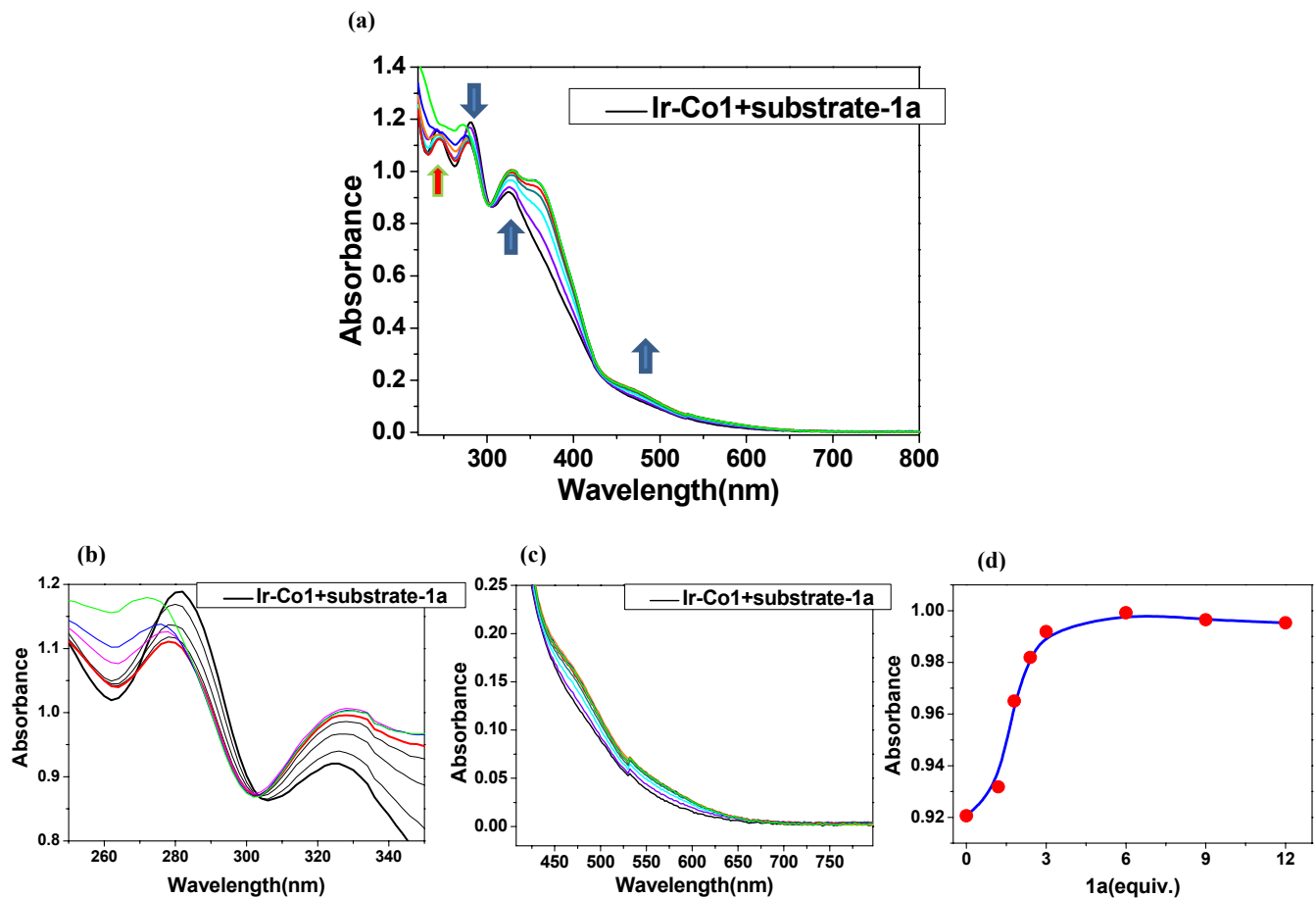


Figure S5 (a) Family of the differentiate UV-vis absorption spectra of **Ir-Co1**(10 μ M, black line) in CH₃CN upon addition of 1.2, 1.8, 2.4, 3.0 equiv. of **1a** (red line) and excess **1a** (6.0 to 12.0 equiv.), respectively; (b) The range of 250-350 nm; (c) The range of 408-798 nm; (d) The UV-vis absorption intensity tracing at 324 nm.

4.4.4 UV-vis titration experiment of Ir-Co2 upon addition of 3.0 to 9.0 equiv. of 1a

When 3.0 to 9.0 equiv. 2-acylpyridine (**1a**) was added to the solution of capsule **Ir-Co2**, the range of 300-800 nm absorbance intensity was not changed and only caused the range 220-280 nm absorbance intensity increased of itself, which indicated that capsule **Ir-Co2** has been lost the substrates bonding activate ability.

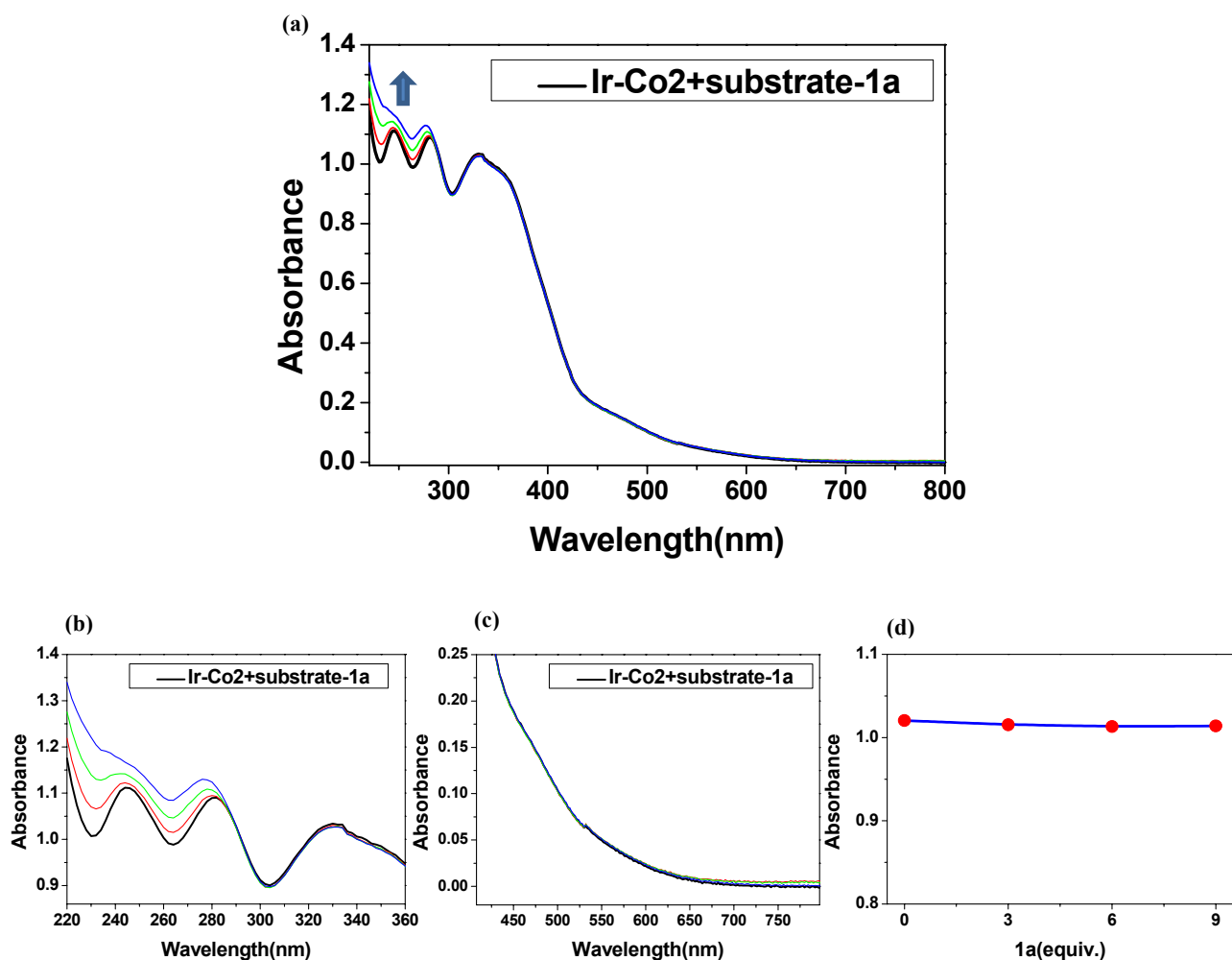


Figure S6 (a) Family of the differentiate UV-vis absorption spectra of **Ir-Co2** (10 μ M, black line) in CH_3CN upon addition of 3.0 to 9.0 equiv. of **1a**, respectively; (b) The range of 220-360 nm; (c) The range of 408-798 nm; (d) The UV-vis absorption intensity tracing at 324 nm.

4.4.5 Possible catalytic mechanism

Based on the above control experiments, the following plausible mechanism is proposed for the formation of the trichloromethylated product in the presence of visible light which is agreed with the reported results^[S3].

Accordingly, the catalytic cycle is initiated by bidentate coordinating of the 2-acylpyridine substrate to the iridium catalyst **Ir-Co1** (intermediate **I**), followed by base-promoted deprotonation to an electron-rich enolate (intermediate **II**). The subsequent addition of a reductively generated electrophilic trichloromethyl radical to the nucleophilic double bond provides cobalt-coordinated ketyl radical (intermediate **III**), which is oxidized to a coordinated product (intermediate **IV**), then products released upon exchange with unreacted starting material, followed by a new catalytic cycle.

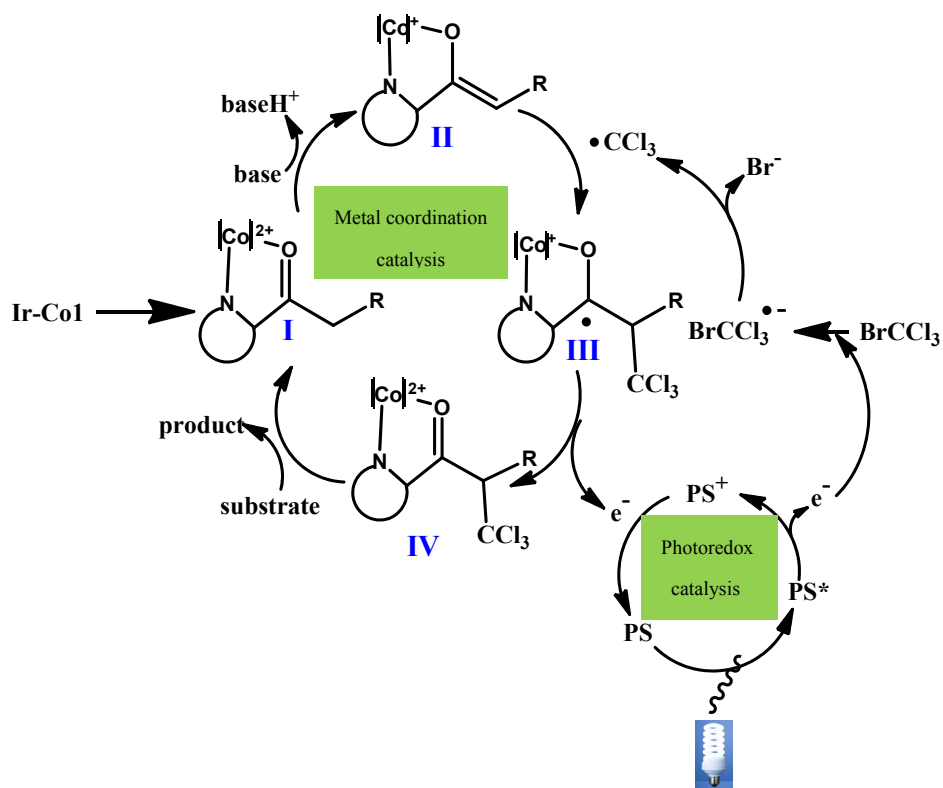


Figure S7 Possible catalytic mechanism

5 Single-Crystal X-Ray Diffraction Studies

5.1 Crystallography

Intensities of the crystal data were collected on a Bruker SMART APEX CCD diffractometer with graphite monochromated Mo-K α ($\lambda = 0.71073 \text{ \AA}$) using the SMART and SAINT programs.^[S4] The structures were solved by direct methods and refined on F^2 by full-matrix least-squaresmethods with SHELXTL version 5.1.^[S5] Crystallographic data have been deposited with the CCDC number being **1481763 and 1481764.**

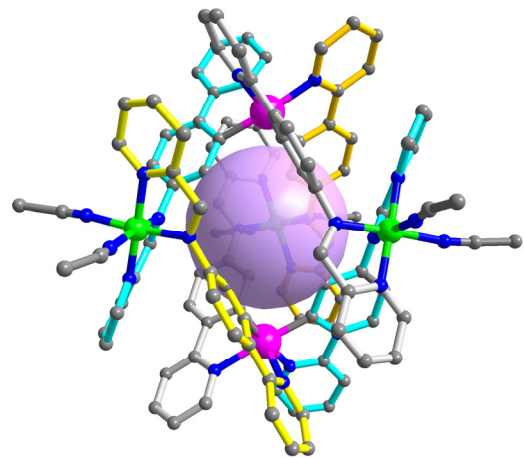
For the crystal data of compound **Ir-Co1**, the non-hydrogen atoms were refined anisotropically. Hydrogen atoms within the ligand backbones and the solvent acetonitrile and diethyl molecules were fixed geometrically at calculated distances and allowed to ride on the parent non-hydrogen atoms. Two oxygen atoms in one of the perchlorates, and the oxygen atom in the solvent diethyl molecule were disordered into two parts with the site occupancy factors (s.o.f.) of each parts being fixed as 0.5, respectively. The adjacent bond distances of the solvent diethyl molecule were restrained to be same.

CCDC No. 1481763.

For the crystal data of compound **Ir-Co2**, except the half occupied the carbonate and the solvent molecules, non-hydrogen atoms in the backbone of the capsule complex were refined anisotropically. Hydrogen atoms within the ligand backbones and the solvent acetonitrile and diethyl molecules were fixed geometrically at calculated distances and allowed to ride on the parent non-hydrogen atoms. The bond distances in one pyridine and one benzene rings of the ligand backbones were retrain as ideal values. **CCDC No. 1481764.**

Table S2 Crystallographic data of compounds **Ir-Co1** and **Ir-Co2**

	Ir-Co1	Ir-Co2
Formula	$\text{Ir}_2\text{Co}_3\text{C}_{118}\text{H}_{108}\text{N}_{24}$ O_{29}Cl_6	$\text{Ir}_2\text{Co}_3\text{C}_{121}\text{H}_{107}\text{N}_{25}$ O_{22}Cl_4
$V(\text{\AA}^3)$	3100.17	2966.31
T/K	200(2)	173(2)
Crystal system	Monoclinic	Tetragonal
Space group	C2/c	P4(3)2(1)2
$a/\text{\AA}$	31.230(5)	20.973(3)
$b/\text{\AA}$	17.481(3)	20.973(3)
$c/\text{\AA}$	26.747(4)	30.067(5)
$\beta (\text{^\circ})$	102.845(2)	90.00
$V/\text{\AA}^3$	14237(4)	13226(4)
Z	4	4
$D_{\text{v}}/\text{g cm}^{-3}$	1.446	1.490
μ/mm^{-1}	2.392	2.529
$F(000)$	6186	5948
No. refs. measured	37130	78149
No. unique refs	12519	11621
R_{int}	0.0818	0.0827
$R_1[I > 2\sigma(I)]$	0.0643	0.0763
wR_2 (all data)	0.1793	0.2056
Goodness of Fit	1.049	1.022
CCDC No.	1481763	1481764



Ir-Co1

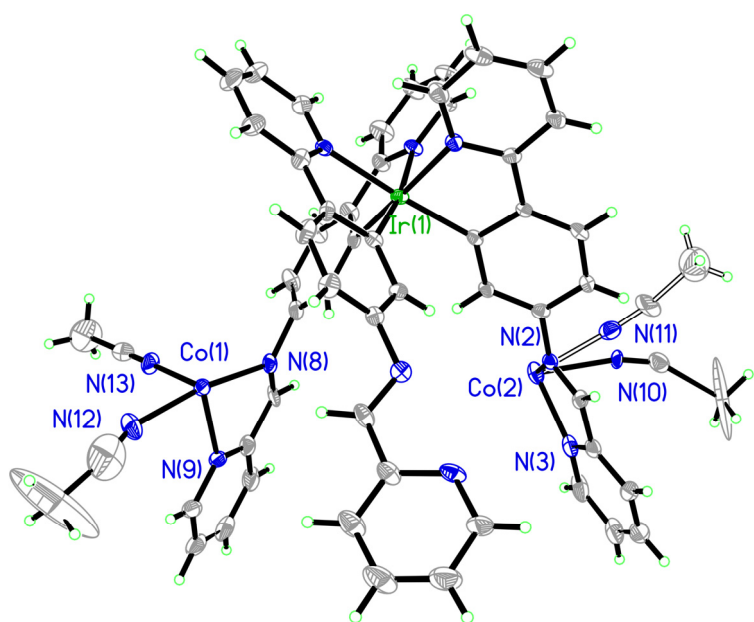
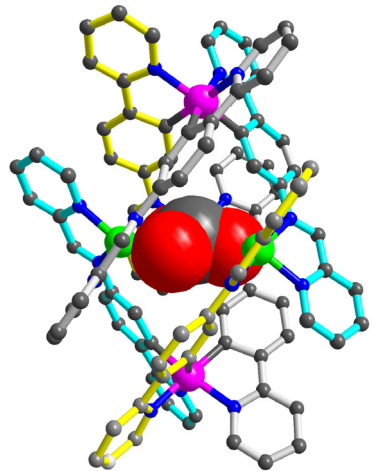


Figure S8 Structure of **Ir-Co1** capsule within an unique asymmetric unit, showing the backbone of the ligands and coordination environment of metal centers in the complex. Selected bond distances (\AA) and angles ($^\circ$): Co(1)-N(12) 2.078(9), Co(1)-N(8) 2.100(7), Co(1)-N(13) 2.107(8), Co(1)-N(9) 2.125(8), Co(2)-N(3) 2.075(9), Co(2)-N(10) 2.109(17), Co(2)-N(2) 2.118(7), Co(2)-N(11) 2.16(2), N(12)-Co(1)-N(8) 168.1(4); N(12)-Co(1)-N(13) 88.7(4), N(8)-Co(1)-N(13) 88.4(3), N(12)-Co(1)-N(9) 90.9(4), N(8)-Co(1)-N(9) 77.4(3), N(13)-Co(1)-N(9) 86.0(3), N(3)-Co(2)-N(10) 78.3(5), N(3)-Co(2)-N(2) 78.6(3), N(10)-Co(2)-N(2) 90.9(6), N(3)-Co(2)-N(11) 96.1(6), N(10)-Co(2)-N(11) 20.8(5), N(2)-Co(2)-N(11) 83.7(6).



Ir-Co2

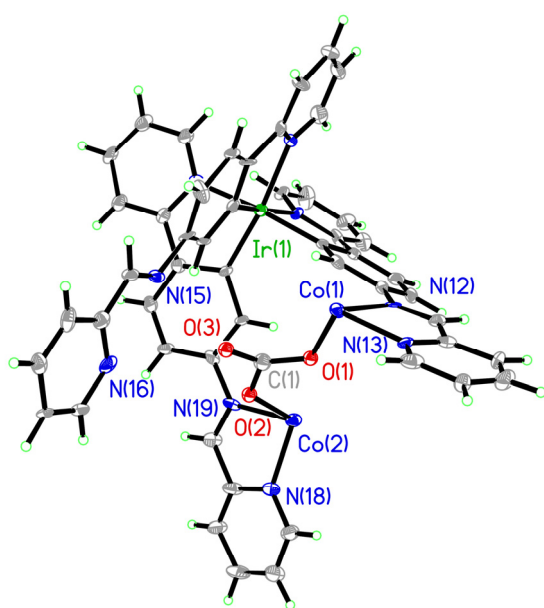


Figure S9 Structure of **Ir-Co2** capsule within an unique asymmetric unit, showing the backbone of the ligands and coordination environment of metal centers in the complex. Selected bond distances (\AA) and angles ($^\circ$): Co(1)-O(1) 1.926(13), Co(1)-N(13) 2.089(7), Co(1)-N(12) 2.149(8), Co(2)-O(2) 1.942(12), Co(2)-N(18) 2.073(8), Co(2)-N(19) 2.118(9), Co(2)-O(2) 1.942(12), C(1)-O(1) 1.313(18), C(1)-O(2) 1.256(19), C(1)-O(3) 1.331(12); O(1)-Co(1)-N(13) 109.3(4), O(1)-Co(1)-N(12) 78.6(4), N(13)-Co(1)-N(12) 78.3(3), O(2)-Co(2)-N(18) 109.9(4), O(2)-Co(2)-N(19) 80.5(4), N(18)-Co(2)-N(19) 78.3(3), O(2)-C(1)-O(1) 121.5(8), O(2)-C(1)-O(3) 115.7(12), O(1)-C(1)-O(3) 115.9(12).

6 ^1H -NMR Spectra

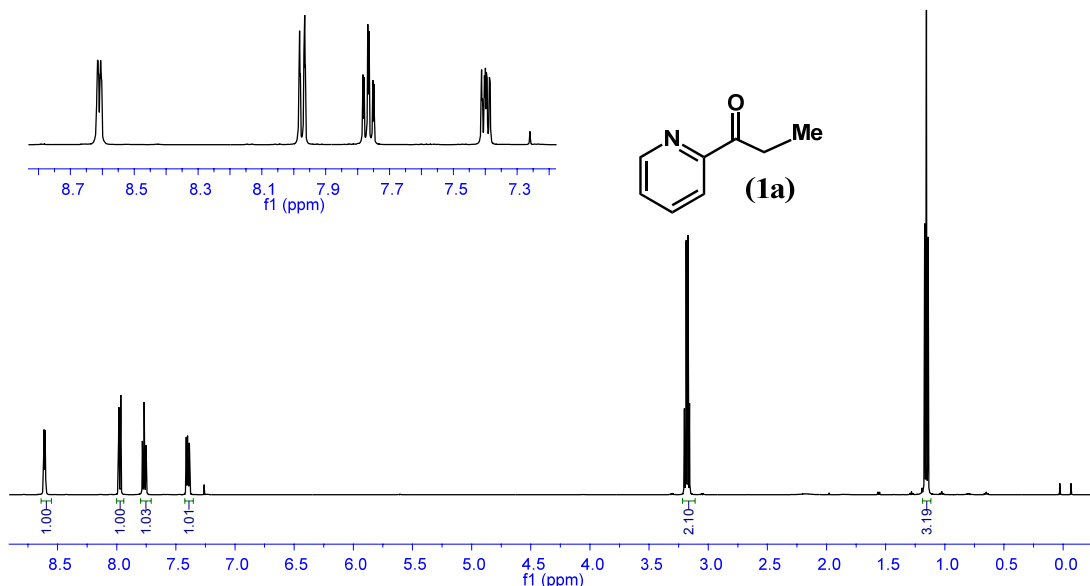


Figure S10 ^1H -NMR spectra of **1a**

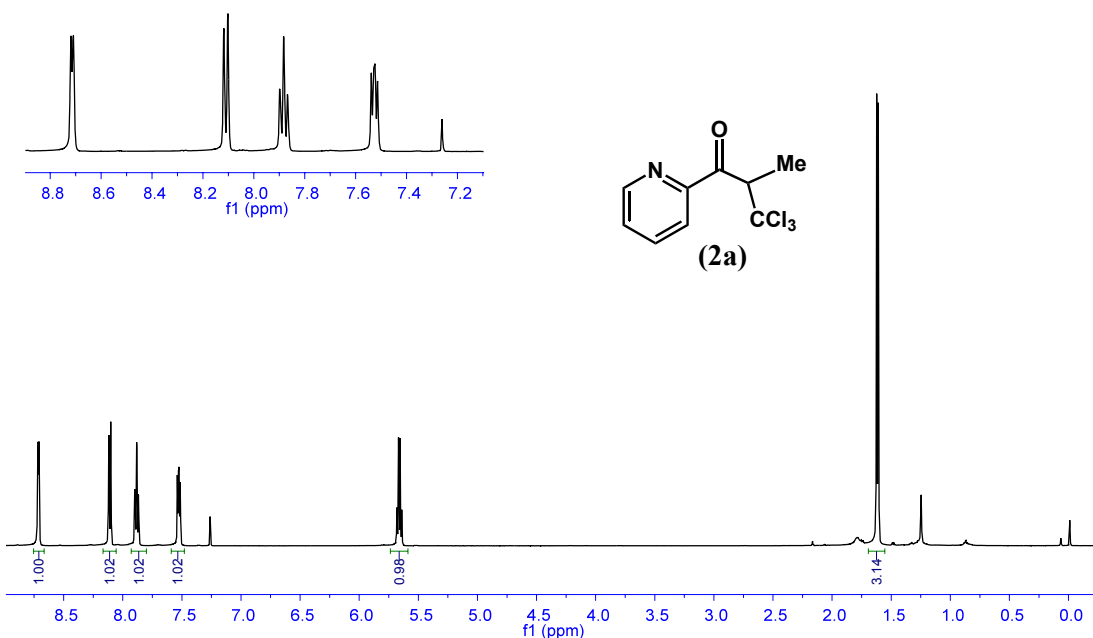


Figure S11 ^1H -NMR spectra of **2a**

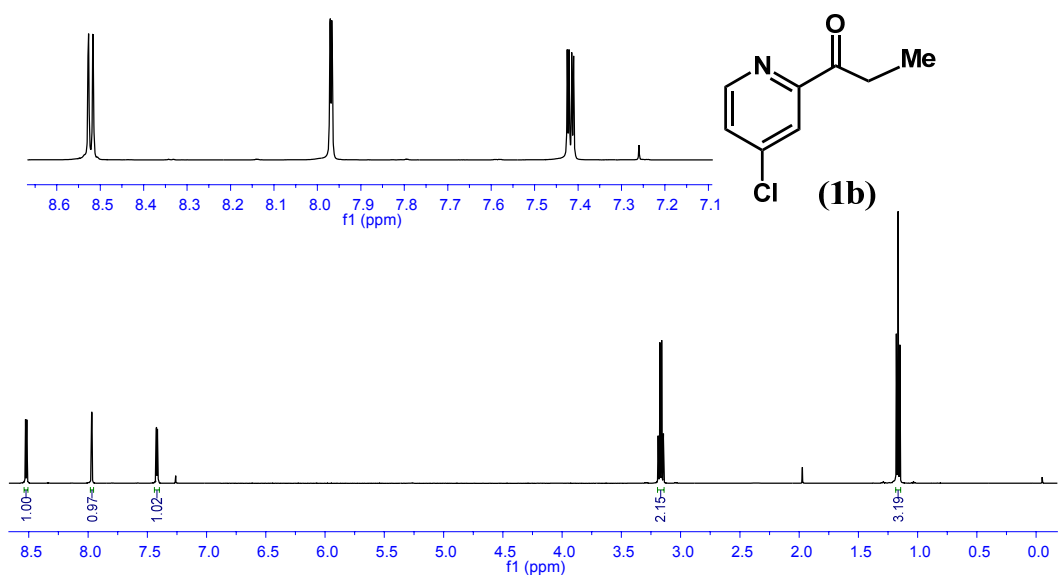


Figure S12 ¹H-NMR spectra of **1b**

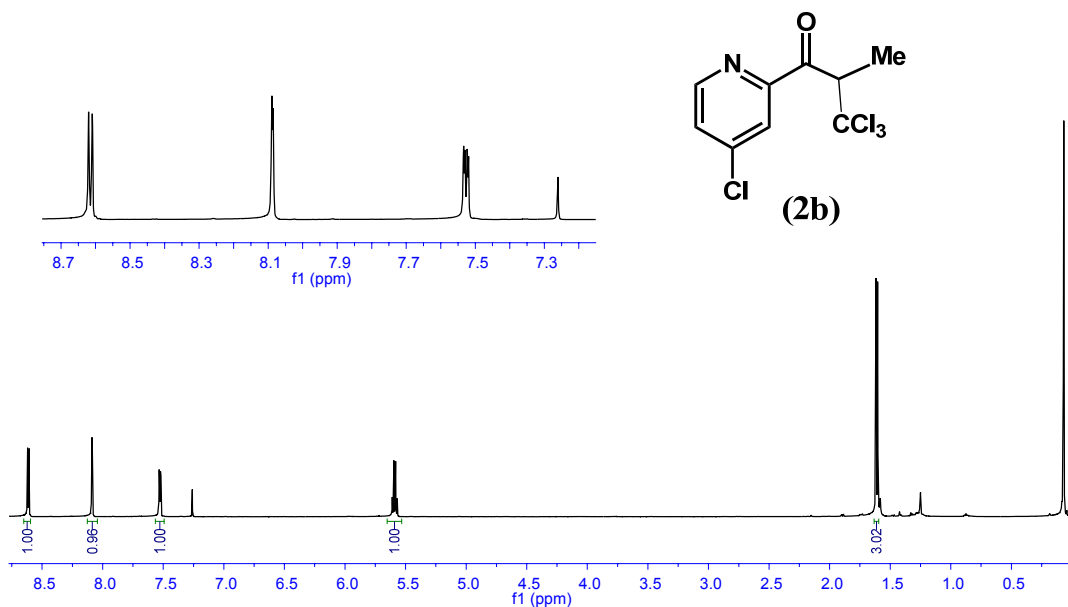


Figure S13 ¹H-NMR spectra of **2b**

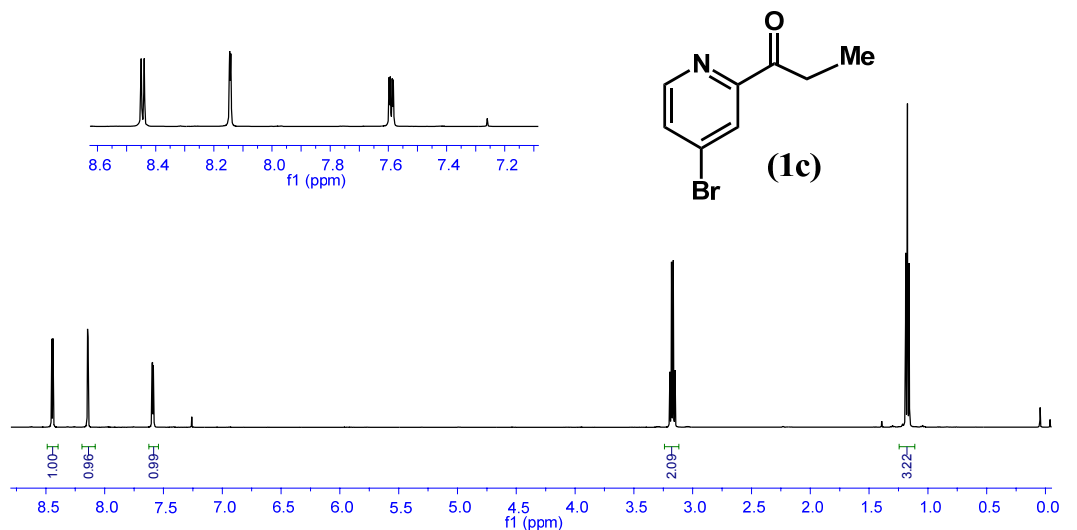


Figure S14 ¹H-NMR spectra of **1c**

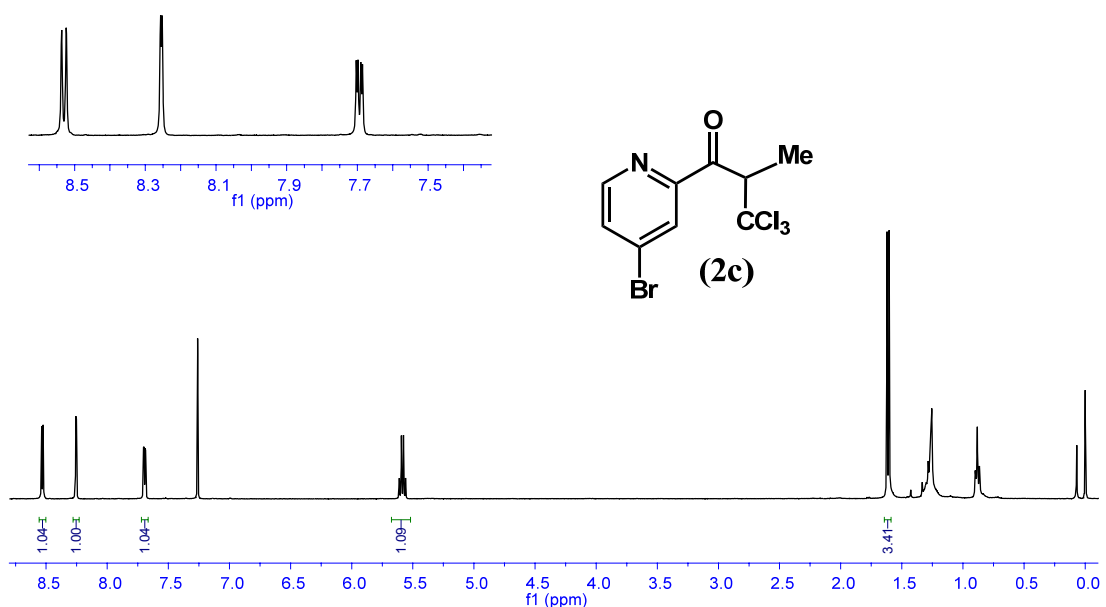


Figure S15 ¹H-NMR spectra of **2c**

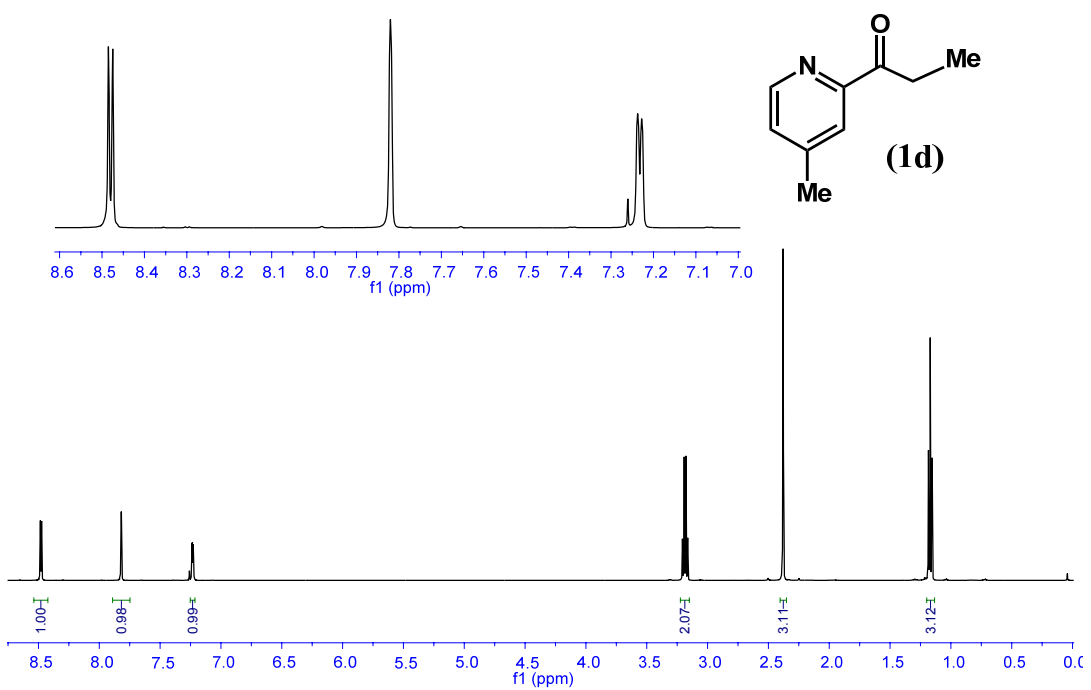


Figure S16 ¹H-NMR spectra of **1d**

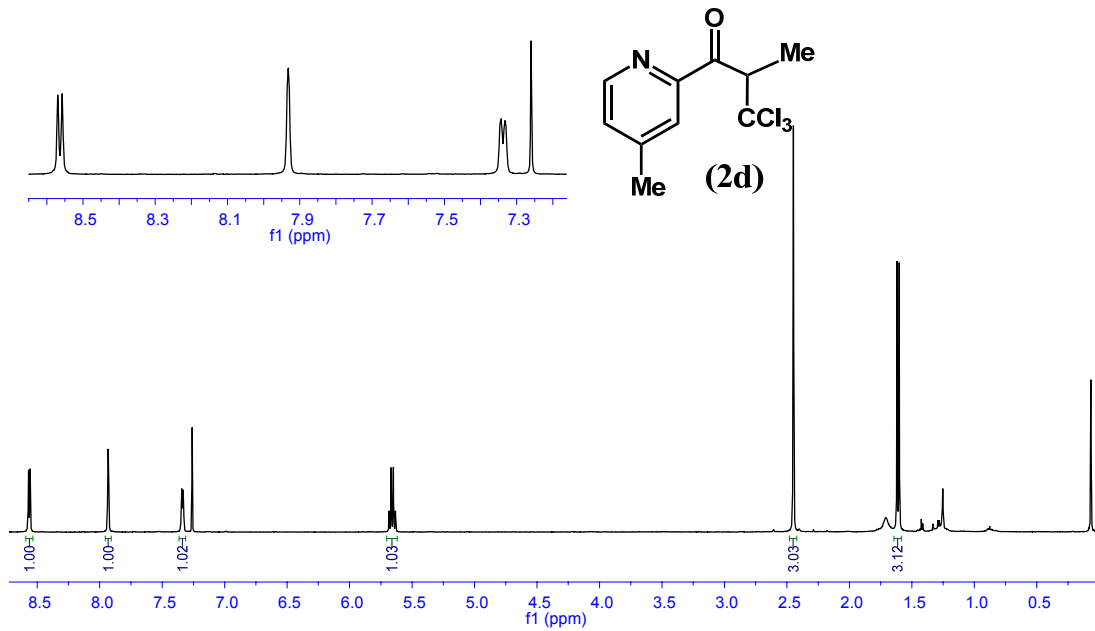


Figure S17 ¹H-NMR spectra of **2d**

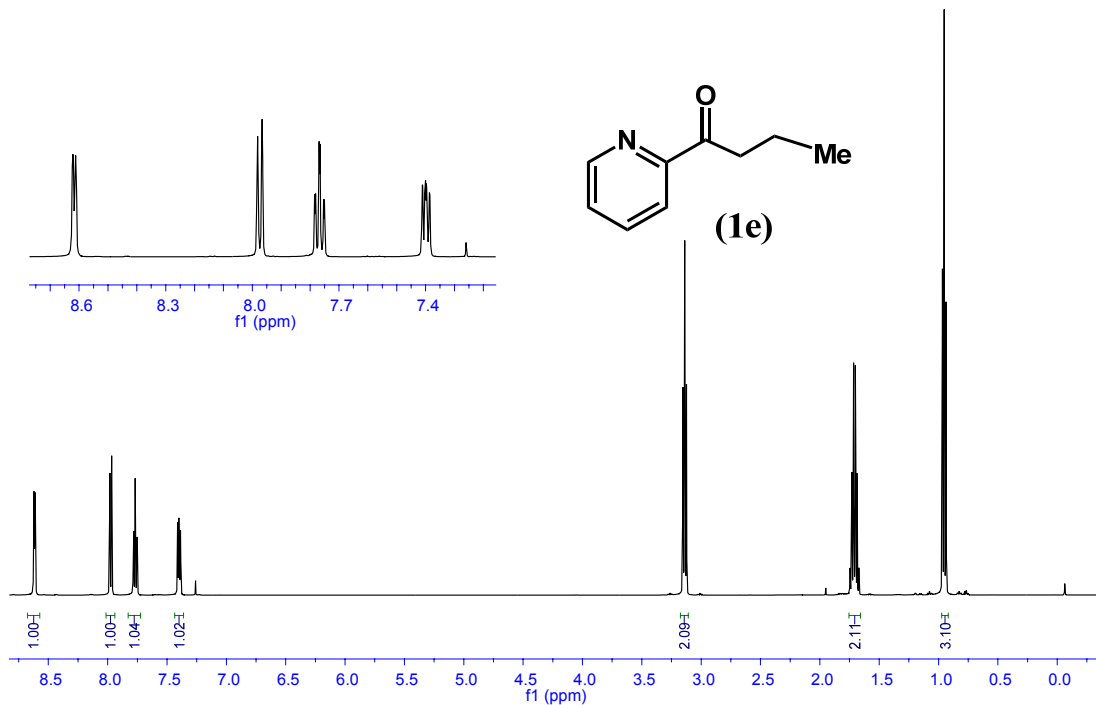


Figure S18 ¹H-NMR spectra of **1e**

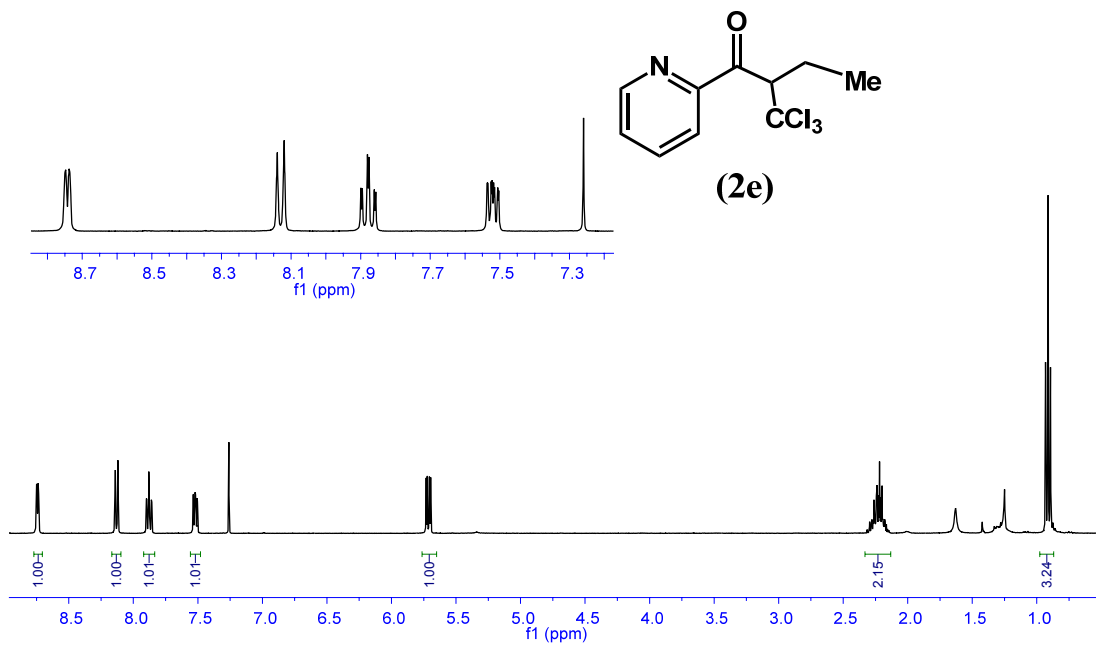


Figure S19 ¹H-NMR spectra of **2e**

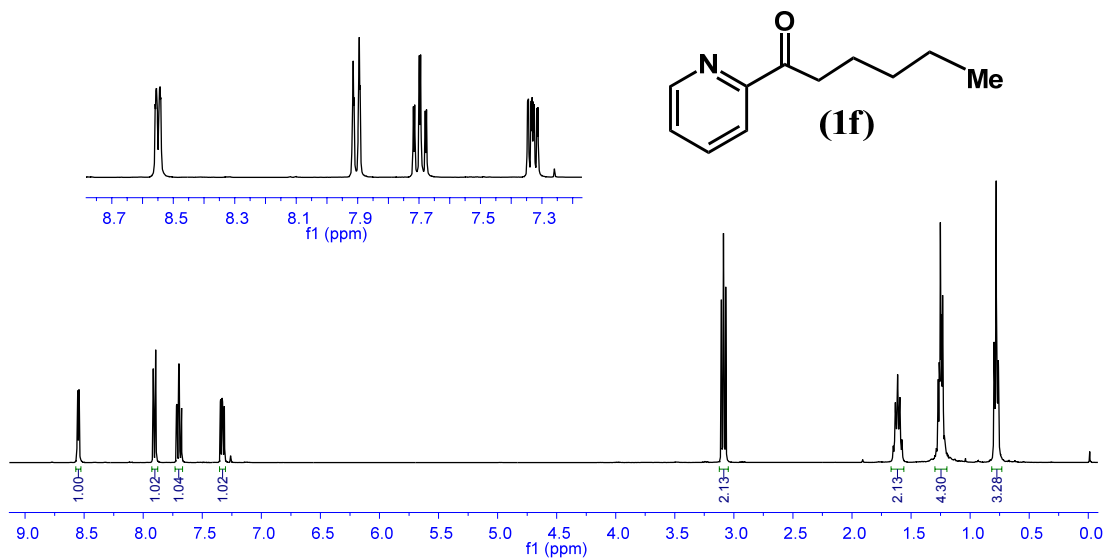


Figure S20 ¹H-NMR spectra of **1f**

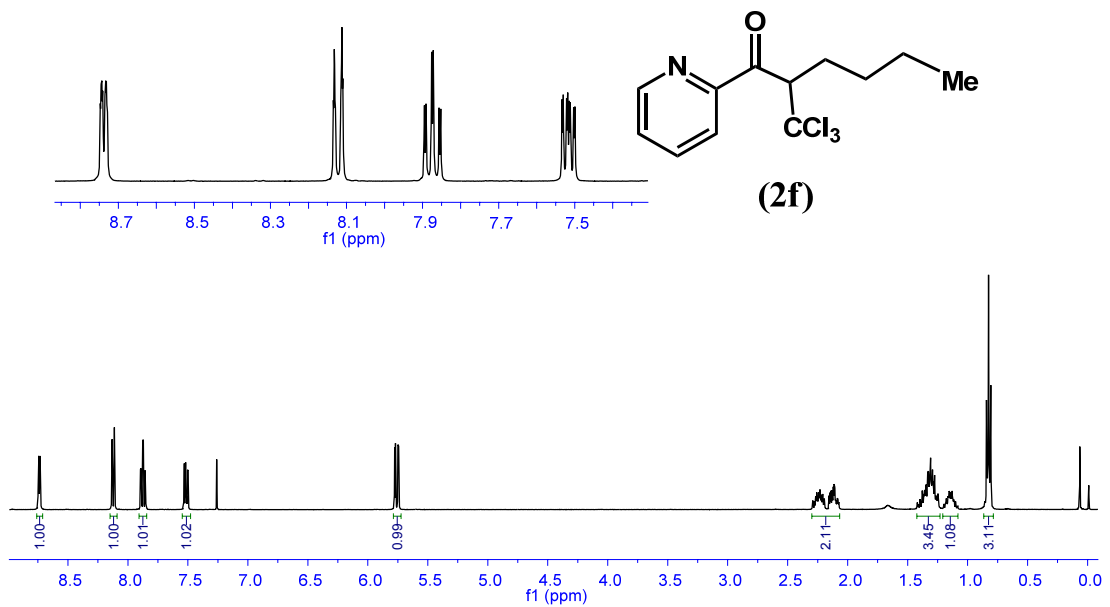


Figure S21 ¹H-NMR spectra of **2f**

7 References

- [S1] X. Z. Li, J. G. Wu, C. He, R. Zhang and C. Y. Duan, *Chem. Commun.*, 2016, **52**, 5104-5107.
- [S2] J. Easmon, G. Purstinger, K. S. Thies, G. Heinisch and J. Hofmann, *J. Med. Chem.*, 2006, **49**, 6343-6350.
- [S3] H. Huo, C. Wang, K. Harms and E. Meggers, *J. Am. Chem. Soc.*, 2015, **137**, 9551-9554.
- [S4] SHELXTL V6.14, Bruker Analytical X-Ray Systems, Madison, WI., 2003.
- [S5] G. M. Sheldrick, SHELXTL V5.1, Software Reference Manual, Bruker, AXS, Inc.: Madison, WI, 1997.